Benchmarking of the Conductance Increment Method and its improved versions

Ismail Isknan[1*], Abdellah Asbayou[1,] Ahmed Ihlal[1] , Lahoussine Bouhouch[1]

[1] *Laboratory of Materials and Renewable Energies, University Ibn Zohr, 80000 Agadir, Morocco.*
[*]*Isknan Ismail. Email: ismail.isknan@edu.uiz.ac.ma*

ABSTRACT

To increase the performance of a photovoltaic (PV) system, a circuit using MPPT (Maximum Power Point Tracking) technology must be used. There are several algorithms proposed in the literature and they need to be compared to select the best performing MPPT technology for a specific application or to make recommendations for future MPPT research. This article presents a benchmarking the most widely used MPPT algorithms, namely the "INC_C" (Classical Incremental Conductance), the "INC_AM" (Modified Adaptive Incremental Conductance). The comparative study presented in this work will confirm that "INC_AM» is the best MPPT technique to improve the efficiency of a PV system.

Keywords: *solar panel; energy; photovoltaic; MPPT technic; Conductance Increment.*

1. INTRODUCTION

The PV energy conversion system must operate near to the maximum power point (MPP) in order to increase solar system efficiency. It is therefore necessary to use MPPT which plays an important role in tracking maximum power points as they maximize the efficiency of the PV system under given conditions and minimize the overall cost of a PV installation [1, 2]. Various MPPT techniques have been developed and used to monitor the MPP of PV systems, such as: the P&O technique [3], which is based on iterative algorithms and is easy to implement but with an inevitable oscillation problem. The Incremental Conductance technique [4]. The Fuzzy Logic Control (FLC) search technique [5], which is used very successfully in the implementation of MPP research, among these existing MPPT control methods, the P&O algorithm, is widely used in many PV systems [6]. The P&O method works well when solar irradiation and temperature do not vary rapidly over time [7], but it cannot quickly keep up with the MPP and therefore the output power oscillates around the MPP. The examination of the Incremental Conductance (INC) approach and its modifications is the subject of this work.

This document is structured as follows: After the introduction, section 2 presents the mathematical model of the PV cell. Section 3 deals with the MPPT technique used to design a Boost Converter. In section 4 we present the simulation results with their discussion to evaluate the algorithm developed, finally, we conclude our work.

2. SOLAR CELL MATHEMATICAL MODEL

Photovoltaic models with one or two diodes have been widely used to model the I-V output characteristic of a photovoltaic cell or panel [8].

The single diode model is the simplest one. It is improved by the incorporation of an Rs series resistor [9]. However, despite its simplicity, it has relatively significant errors compared to experimental data when exposed to high temperature variations. Model optimization is achieved by including an additional shunt resistor Rsh [10]. In addition, its accuracy decreases at low irradiance, especially in the open circuit voltage range Voc.

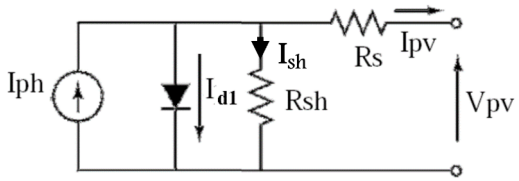

Figure 1: One diode equivalent circuit of a PV cell.

The electrical current of the PV panel for the one diodes model is given by: [11, 12]

$$I_{pv} = I_{ph} - I_{d1} - I_{sh} \quad (1)$$

So, The following relation describes the current supplied by a solar cell in a single diode model : [13,14]

$$I_{pv} = I_{ph} - I_{01}\left[exp\left(\frac{V_{pv} + R_s I_{pv}}{n_1 V_{th}}\right) - 1\right] - \frac{V_{pv} + R_s I_{pv}}{R_{sh}} \quad (2)$$

With:

I_{ph} Photo-generated current (A).
Ipv Solar cell terminal current (A).
I_{0i} Reverse saturation current of diode in conventional model (A).
R_S Series resistance (Rs).
R_{sh} Shunt resistance (Rsh).
V_{pv} Solar cell output voltage (V).
$V_{th} = \frac{k\,T}{q}$ Thermal voltage (V).
n_1 The ideality factors

3. TECHNIQUE MPPT

The characteristics of the generator I (V) depend on the illumination and temperature "add reference". The maximum power point fluctuates as a result of these climatic variations. Due to these fluctuations, we often insert one or more controlled static converters that can follow the maximum power point.
These commands are called MPPT and are associated with the chopper controls to ensure the coupling between the PV generator and the receiver by forcing the former to provide its maximum power.

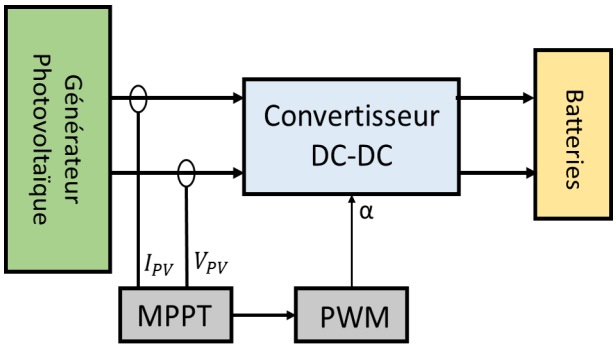

Figure 2: Synoptic diagram of the PV system studied

As illustrated in Figure 2, the proposed framework comprises of a PV panel, a DC-DC converter lift, equipped with its MPPT control block and a battery. The MPPT control block ensures, under certain conditions, the control of the conduction and blocking of the MOSFET by changing the duty cycle α of the PWM signal driving this MOSFET.

The specifications of the PV module used (XXR-SFSP-H50-62W) [15] are given in Table 1.

Table 1: SPECIFICATIONS of the PV module used in Matlab / Simulink

Parameter	Symbol	Value
Maximum power(W)	P_{mp}	63
Open circuit voltage(V)	In_{OC}	14.5
Short circuit current(A)	I_{SC}	5.5
Voltage at maximum power point(V)	V_{mp}	11.9
Current at maximum power point(A)	I_{mp}	5.3
Number of PV cells per module	N_{cell}	22

The specifications of the booster chopper converter used are summarized in Table 2:

Table 2: Lift Chopper Specifications

Parameter	Symbol	Value
Switching frequency (kHz)	F	30
Booster inductance (µH)	L	330
Input capacitor (µF)	C	100

Table 3 lists the specs of the battery that was utilized as a charge at the converter's output:

Table 3: Specifications of the battery used

Parameter	Symbol	Value
Rated voltage(V)	In_n	48
Rated capacity(Ah)	C_n	10
Initial state of charge (%)	SOC	10

Figure 3 shows the irradiation profile employed during a period of 0.3 s at a constant temperature of 25 C. Fig. 4 shows the highest power related to the irradiation setup used. The power supplied by the PV panel under the chosen irradiation and temperature profile corresponds to the power delivered by the PV panel under the environmental parameters imposed by the chosen irradiation and temperature profile.

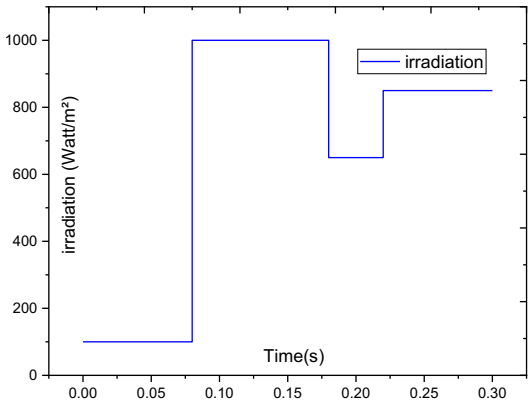

Figure 3: Irradiation profile used in simulation

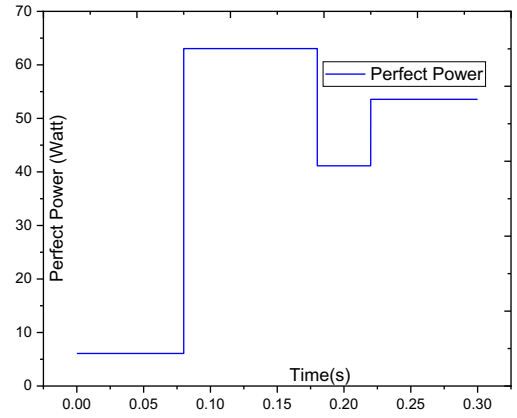

Figure 4: Ideal power of the system used in Matlab / Simulink

3.1. Method "Classic Conductance Increment" (INC_C)

The steady conductance was planned based on a perception of the trademark bend P(V). This calculation was created in 1993 and meant to conquer a portion of the hindrances of the P&O calculation [16]. This method depends on the information on the conductance of the PV module and the results on the working point according to the greatest force point (MPP). Accordingly, the conductance Gc of the PV not really settled in the connection between the current and the yield voltage of the PV module demonstrated underneath.

$$G_c = \frac{I}{V} \tag{3}$$

So an elementary variation (Increment) of the conductance can be defined by:

$$dG_c = \frac{dI}{dV} \tag{4}$$

Furthermore, the advancement of the force of the PV module corresponding to the voltage gives the situation of the working point according to the MPP. When the force subordinate is zero, we are on the MPP; if it is positive, the working point is to the left of the highest worth; if it is negative, the working point is to the right. The following situations are shown in Figures 5(a) and 5(b):

$$\frac{dP}{dV} = I + V.\frac{dI}{dV} \tag{5}$$

Let Vpv be the voltage at the PV module's output and Vmpp be the voltage at the PV module's maximum power point [17] [18]. The derivative dP/dV in this example can meet the following conditions:

- If dP/dV > 0, the operating point is to the left of the MPP, $V_{mpp} > V_{pv.}$
- If dP/dV < 0, the operating point is to the right of the MPP, $V_{mpp} < V_{pv.}$
- If dP/dV = 0, the operating point is on the MPP, $V_{mpp} = V_{pv}$.

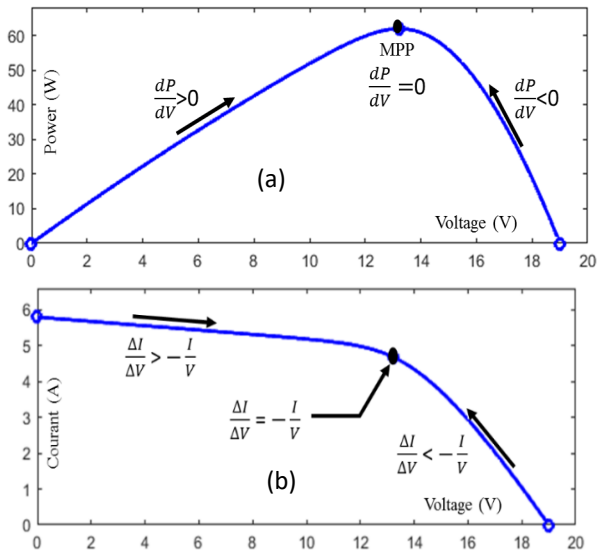

Figure 5: Positioning of the (a) operating point according to the sign of the derivative of the conductivity Gc and (b) the power P

Regarding this INC_C technique, the organizational chart presented in Figure 6 explains the different stages of its implementation. The quantity Vref visible in this flowchart is the reference voltage for which the PV panel is forced to operate. Once the MPP is reached, the corresponding operating point is maintained, unless a change of ΔI is noted, indicating a change in atmospheric conditions and therefore in MPP. The algorithm then increases or decreases Vref to search for the new MPP.

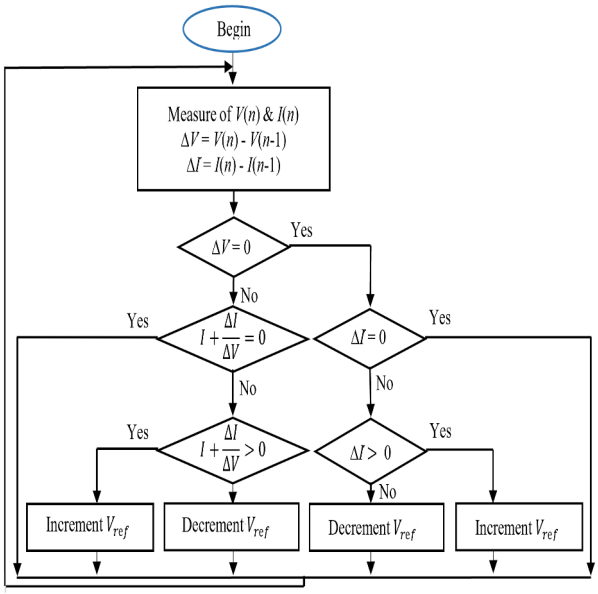

Figure 6: Algorithm associated with method INC_C [19].

Under the climatic conditions mentioned at the beginning of this work, Figure 7 summarizes the simulation results of the

algorithm INC_C under Matlab / Simulink. In this figure, we find essentially 3 curves spread over an interval of 0.3 s: the first representing the voltage Vmpp_INC output of the PV module, the second corresponding to the current Impp_INC of the PV panel, and finally the third representing the power Pmpp_INC of the PV module.

The results of Figure 7 show that the PV model with the algorithm "INC_C" converges to the desired optimal values with oscillations around the MPP (Zoom 2), The performance of the algorithm is rigid and good. The response to a rapid variation (Zoom 1) is done in a fluid way at around 0.075 s, corresponding to the passage of the irradiation from 100 W/m2 to 1000 W/m2, as well as the satisfactory monitoring of the MPP under different lighting conditions.

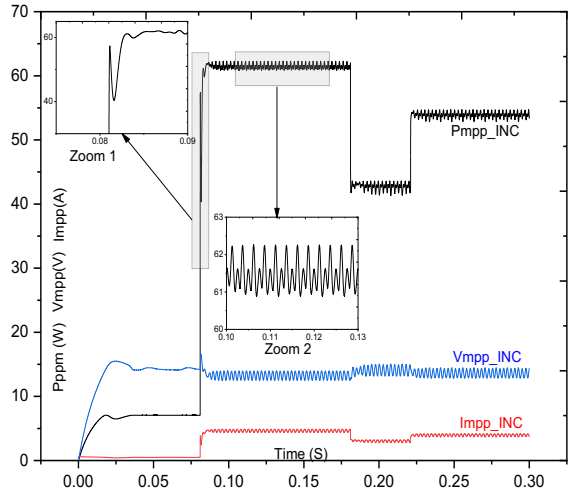

Figure 7: Response in terms of PV module power with the "INC_C" algorithm

3.2. Method "Increment of Adaptive Conductance Modifiede" (INC_AM)

The processing is separated into two sections in this technique, each of which is critical for detecting the target MPP value. The first section addresses the discrepancy between tracking precision and convergence speed. The second half, on the other hand, provides for the removal of the influence of drift during a quick change in light.

- Part One:

Given the contradictions between the accuracy of the tracking and the speed of convergence of the "INC_C", we present here in the first part of our improved adaptive algorithm, namely the "INC_AM" variable-step method. When the operating point is further away from the MPP, the primary principle is to pick a step high enough to speed up the optimization. When it's getting close to the MPP, you'll want to pick a tiny enough step to emphasize precision.

As illustrated in Figure 8, the P(V) curve is separated into three portions (1, 2 and 3). Let k = dP / dV, the slope at a point n of this curve; in zone (1), k is basically positive, and in zone (3) it is negative. In addition, the absolute value of k in zones (1) and (2) is greater than its absolute value in zone (3). The operating point can be determined according to the sign of k. When k > 0, essentially in zone (1), the disturbance can be set larger (d1). When k < 0 (zone 3), we can choose a small perturbation step (d2). When | k | < ε while tending towards 0, the system works in the region (2), corresponding to an operation around the MPP i.e. ε | dV | - | dP | > 0. In this case, all we need to do now is address a little stumbling block (d3). The flowchart of the first portion of the "INC AM" algorithm in Figure 9 illustrates this principle of action.

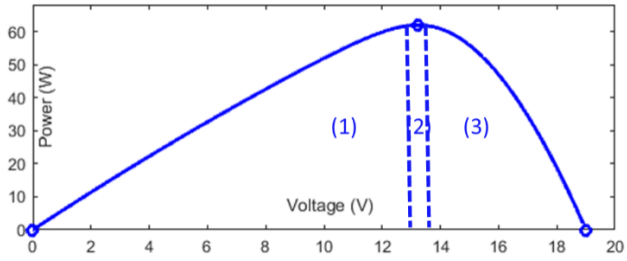

Figure 8: P(V) characteristics of the PV module

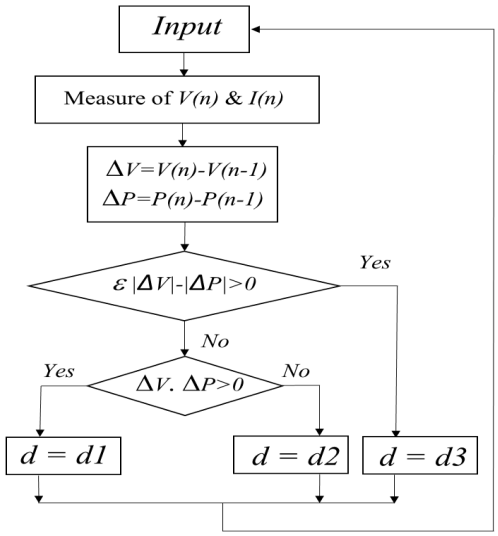

Figure 9: The first part of the"INC_AM" algorithm flowchart

- Part Two:

The PV module's maximum usable power is determined by the ambient temperature and the amount of solar irradiation. Figure 10 depicts two PV module characteristic curves: I (V) and P (P) (V). These graphs are used to investigate the impact of sun radiation. and temperature on the power output of the PV module. When a load is connected to the PV module, a load line is placed on the curve I (V). The voltage and current of the PV module are located at the point of intersection of the load line with the curve I (V). The power produced by this module can thus be calculated simply by multiplying the current by the voltage at the place where this load line intersects the curve I. (V). The load line's location on curve I (V) is determined by the

impedance of the load.

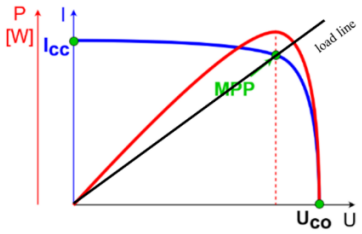

Figure 10: Characteristics I (V) and P(V) of a PV module.

The algorithm of INC_C exploit the slope of the P (V) curve to detect the MPP. If the algorithm finds that the operating point is at the top of the curve P (V), corresponding to a slope is zero, and equation (6) is satisfied, then the duty cycle α of the DC-DC converter is fixed and no oscillation occurs during this step until changes in the slope occur. In real life, the zero slope condition is rarely reached.

Generally, the algorithm INC_C fails to make a good decision when the irradiation is suddenly increased [20], as shown in Figure 11. Indeed, when the irradiation is at 0.3 kW/m², the MPPT algorithm adjusts the duty cycle to ensure that the PV system operates on the load line 2 and that the MPP (point B) is tracked. After some time, solar irradiation may increase to 1 kW/m², but the duty cycle is maintained at charge line 2. Therefore, the point M will be recorded by the load line 2 on curve I(V), corresponding to the power at point C on the curve P(V). Therefore, the algorithm of INC_C calculates the slope between point C and point B, which is then positive. However, the charge line 2 detects power at point C, which is coupled with a negative slope between point C and point A, which is the genuine MPP. As a result, the algorithm INC C increases the output voltage of the PV module without detecting the anomaly, causing the PV module's power to drift away from the real MPP.

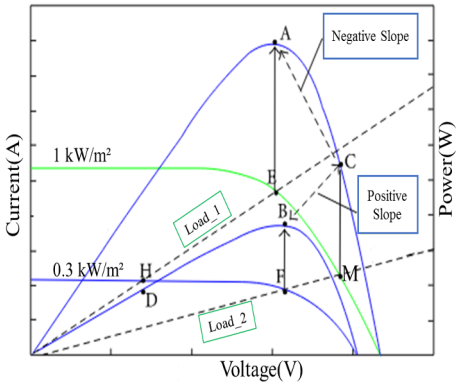

Figure 11: P-V and I-V curves for solar irradiation of 300 W/m2 and 1000 W/m²

Subsequently, based on the value of the change step dx determined by the first part of the algorithm, we can estimate the adequate value of the duty cycle α:
Based on the above analysis, the second part of the algorithm of INC_AM is illustrated in Figure 12. Initially, the variable β is set to zero. The value of β is used to indicate that the MPP is reached when this β is 1. Otherwise, the variable β remains equal to 0, and the INC_C algorithm is implemented with the use of the following equation:

$$\left|\frac{I}{V}+\frac{dI}{dV}\right| < 0.06 \qquad (6)$$

When the condition of equation (6) is met, the system operates in MPP. Therefore, the algorithm sets β to 1 and then switches to the improved algorithm.

In the improved adaptive algorithm, the program continues to check the state of the equation (6). If solar radiation and charge remain constant, the duty cycle α will not change. When solar radiation changes, the algorithm sets the variable β to zero. The program then analyses the fluctuations in the PV module's voltage and output current. If the algorithm detects an increase in current or voltage, the duty cycle will rise as well.

Under the conditions mentioned at the beginning of this work, the result of the simulations of the algorithm "INC_AM" under Matlab / Simulink, are illustrated in Figure 13. The latter is composed of three graphs in a time interval of 0.3 s: The first represents the voltage Vmpp_INC_AM of PV output, the second corresponds to the output current Impp_INC_AM of the PV panel, and the third represents the power Pmpp_INC_AM produced by the PV module.

The results of Figure 13, show that for a rapid variation in the level of solar irradiation, the algorithm "INC_AM" responds better than the algorithm "INC_C", moreover, when the MPP is reached the oscillations in steady state no longer occur.

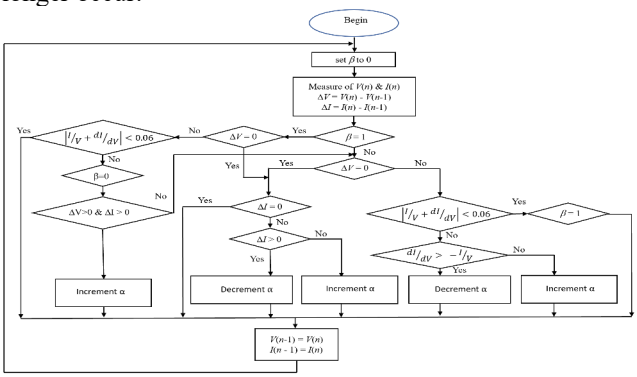

Figure 12: The second part of theAlgorithm associated with the method"INC_AM"

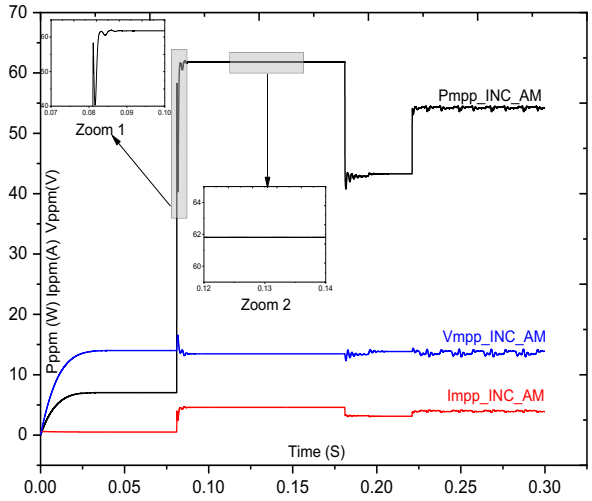

Figure 13: Response in terms of pv module power in the case of the "INC_AM" algorithm

4. COMPARISON OF THE PERFORMANCE OF PROCESSED MPPT ALGORITHMS

In order to ensure a sufficient comparative study between the MPPT algorithms treated, we evaluated certain performance parameters, namely; for each of the two algorithms, the convergence time τc and the oscillation deviation εo for an irradiation ranging from 100 to 1000 W/m2 for each of the two algorithms. The calculation results are reported in the following table:

Table 4: Calculated Performance Parameters

MPPT method	Convergence Time τ_c (ms)	Oscillation deviation ε_o (W)
1 : "INC_C"	31	1.18
2 : "INC_AM"	16	0.01

5. CONCLUSION

In this work dedicated to the study of MPPT methods, we began by exposing the most commonly used method which is "classical incremental conductance" (INC_C) and its improved version: "modified adaptive incremental conductance" (INC_AM). These technologies have easy-to-implement algorithms to control booster-type DC-DC converters.

Generally speaking, the traditional algorithm (INC_C) gives good results, but has big disadvantages. In order to overcome these problems, the improved version of this algorithm has been studied. For the purpose of evaluating the performance of these two algorithms "INC_C" and "INC_AM", we compared their convergence times τc,as well as their oscillation differences εo induced by their use. This allows us to understand and analyze the pros and cons of each of the two methods. It can then be concluded that, compared to the "INC_C" method, the "INC_AM" method is the best with aconvergence time τc lower; 16 msagainst 31 s, with a deviation of oscillation εo very minimized to the value of 0.01 W against 1.18 W.

6. REFERENCES

[1] S. Motahhir, A. El Ghzizal, S. Sebti, and A. Derouich, “Proposal and implementation of a novel perturb and observe algorithm using embedded software,” in 2015 3rd International Renewable and Sustainable Energy Conference (IRSEC), pp. 1–5, Marrakech, Morocco, December 2015

[2] N. Yıldıran and E. Tacer, “Identification of photovoltaic cell single diode discrete model parameters based on datasheet values,” Solar Energy, vol. 127, pp. 175–183, 2016

[3] N. Femia, G. Petrone, G.Spagnuolo, M. Itelli, "Optimization of Perturb and Observe Maximum Power Point Tracking Method", *IEEE Transactions on Power Electronics*, 20(4), 2005, pp. 963-973, doi:10.1109/tpel.2005.850975.

[4] A. Zegaoui, M. Aillerie, P. Petit, J.P. Sawicki, A. Jaafar, C. Salame, J.P. Charles, "Comparison of two common maximum power point trackers by simulating of PV generators", *Energy Proceedia*, 6, 2011, pp. 678–687.

[5] A. Messai, A. Mellit, A. Guessoum, S.A. Kalogirou, "Maximum power point tracking using a GA optimized fuzzy logic controller and its FPGA implementation", *Solar Energy*, 85, 2011, pp. 265–277.

[6] J. Ahmed and Z. Salam, “A modified P&O maximum power point tracking method with reduced steady-state oscillation and improved tracking efficiency,” IEEE Transactions on Sustainable Energy, vol. 7, no. 4, pp. 1506–1515, 2016.

[7] H. Yatimi, E. Aroudam, "Assessment and control of a photovoltaic energy storage system based on the robust sliding mode MPPT controller", *Solar Energy*, 139, 2016, pp. 557-568.

[8] J. J. Soon, K.-S. Low, Shu Ting Goh, "Multi-dimension Diode Photovoltaic Model for

Different PV Cell Technologies", IEEE 23rd International Symposium on Industrial Electronics (ISIE), Turkey, 1-4 June, 2014.

[9] M. Azzouzi, D. Popescu, M. Bouchahdane, "Modeling of Electrical Characteristics of Photovoltaic Cell Considering Single-Diode Model", *Journal of Clean Energy Technologies*, vol. 4, no. 6, 2016, pp. 414-420.

[10] M. R. Rashel, A. Albino, A. Veiga, T. Ahmed, M. Tlemcani, T. C. F. Goncalves, "Comparison of Photovoltaic panel's standard and simplified models", International Conference for Students on Applied Engineering (ISCAE), Newcastle upon Tyne, UK, 20-21 Oct. 2016.

[11] A. Asbayou, M. Agdam, A. Aamoume, A. Soussi, A. Ihlal, L. Bouhouch, "Utilization of MOSFET transistor as an electronic load to trace I-V and P-V curve of a solar panel", *The 3rd International Conference of Computer Science and Renewable Energy* (ICCSRE'2020), 22-24 dec, Agadir, Morocco, 2020.

[12] S. M. Hassan Hosseini, A.A Keymanesh, "Design and construction of photovoltaic simulator based on dual-diode model", *Solar Energy*, vol. 137, 2016, pp. 594-607.

[13] K. Ishaque, Zainal Salam, Hamed Taheri, "Simple fast and accurate two-diode model for photovoltaic modules", *Solar Energy Materials & Solar cells*, vol. 95, 2011, pp. 586-594.

[14] A. Asbayou, A. Aamoume, M. Elyaqouti, A. Ihlal, and L. Bouhouch, "Benchmarking study between capacitive and electronic load technic to track I-V and P-V of a solar panel", *International Journal of Electrical and Computer Engineering (IJECE)*, vol. 12, no. 1, pp. 102–113, 2021

[15] Datasheet of solar panel XXR-SFSP-H50-62W, available online https://enfsolar.com/pv/panel-datasheet/crystalline/42960

[16] Cabal Cedric « Optimisation énergétique de l'étage d'adaptation électronique dédié à la conversion photovoltaïque ». Thèse de doctorat, Université de Toulouse, 2008

[17] Dhananjay Choudhary Int. Journal of Engineering Research and Applications ISSN : 2248-9622, Vol. 4, Issue 8(Version 6), August 2014, pp.123-132

[18] Kumar, H., & Tripathi, R. K. (2012). Simulation of variable incremental conductance method with direct control method using boost converter. 2012 Students Conference on Engineering and Systems. doi:10.1109/sces.2012.6199050

[19] S. Motahhir, A. El Ghzizal, S. Sebti, A. Derouich, "Modeling a photovoltaic system with modified incremental conductance algorithm for rapid irradiance changes", *International Journal of Photoenergy*, 2018, 1-13, doi: 10.1155/2018/3286479.

[20] K. S. Tey and S. Mekhilef, "Modified incremental conductance MPPT algorithm to mitigate inaccurate responses under fast changing solar irradiation level," Solar Energy, vol. 101, pp. 333–342, 2014